SHIP VISCOUS FLOW
A REPORT ON THE 1990 SSPA-CTH-IIHR Workshop

Virendra C. Patel
Iowa Institute of Hydraulic Research
Iowa City, Iowa

Lars Larsson
Chalmers University of Technology and
FLOWTECH International AB
Gothenburg, Sweden

Abstract

To assess the state of the art in ship viscous flow computation a Workshop was organized in 1990 by three organizations: SSPA Maritime Consulting AB, Chalmers University of Technology and Iowa Institute of Hydraulic Research. Two test cases were specified by the organizers and sent out to all interested research groups, which were asked to submit results in a prescribed format. In Septemer 1990 a meeting was held at Chalmers University of Technology. All results had then been collected and presented in a common format, and the theories behind the methods compiled in a table based on responses to a questionnaire sent our earlier. During the meeting, each research group was first given the opportunity to briefly introduce their method and results. Thereafter, a considerable time was spent on general discussions on the performance of the different methods considering the differences in the underlying theories. Specific items that were adressed were grid generation, governing equations, boundary conditions, turbulence modelling and numerical method. Practical aspects on the results, for instance from the point of view of propeller design, were also discussed. The Workshop Proceedings contain a description of the participating methods and the results of both test cases. In the present paper a summary of the Workshop and its results is presented.

Introduction

Although viscosity is present in the entire flow around a ship it has a significant effect only in the boundary layer around the ship and the wake behind it. The present paper deals with the flow in these two regions, which are limited in size, but very important from at least two points of view. Frictional forces within the boundary layer give rise to a viscous resistance of the ship, in most cases the dominant resistance component, and the velocity distribution in the near wake determines the design and performance of the propeller.

Despite its obvious importance the first serious attempts to compute the viscous flow were made relatively recently, about twenty years ago. This is in contrast to the long term research in the inviscid flow area, where wave resistance research has been under way during the entire twentieth century. The reason for the diffe-

rence is that the complicated viscous flow equations, i.e. the Navier-Stokes equations and approximations thereof, are less amenable to analytical treatment than the inviscid equations, normally based on potential flow theory. Therefore it was not until computers had become powerful enough to handle three-dimensional boundary layer theory numerically that research on viscous flow computations was started.

During the 1970's a number of methods for predicting ship boundary layers were developed, and in 1980 it was considered appropriate to assess the state of the art in this area. To accomplish this, an international Workshop on ship boundary layers was organized by SSPA, the Swedish State Shipbuilding Experimental Tank, in cooperation with the International Towing Tank Conference, ITTC[1]. The purpose was to bring together specialists on ship boundary layer calculations from all over the world, and to let them apply their techniques and methods to two test cases, specified in detail by the organizers. In June of 1980 a meeting was held in Gothenburg. The results of 17 methods had then been collected and presented in a uniform format. During the meeting the various components of the methods were discussed in the light of the results produced. The general finding was that most methods were able to predict the thin boundary layer over the major part of the hull with an accuracy sufficient for engineering purposes, while all of the methods failed completely in predicting the flow near the stern and in the wake.

In the 1980's development accelerated, and the focus was changed from the thin boundary layer to the stern/wake flow. As evidenced by the 1980 Workshop a new class of methods with less restrictive approximations was required. The interest of researchers was soon focused on the Reynolds Averaged Navier-Stokes (RANS) equations, and a number of such methods was proposed during the 1980's. Towards the end of the decade it was considered timely to organize a second Workshop to investigate the progress made. This task was undertaken by three organizations: SSPA Maritime Consulting and Chalmers University of Technology (CTH) in Sweden and Iowa Institute of Hydraulic Research (IIHR) in the USA.

As in the first Workshop, the purpose of the new event was twofold:

o   to assess the state of the art in ship
     viscous flow calculations

o   to analyze the results of the diffe-
     rent methods in light of the under-
     lying theories, thereby obtaining
     information on the most promising ways
     to achieve further improvement

     The 1980 Workshop had been successful
in achieving these goals, so the new Work-
shop was organized in a similar way. Two
test cases were selected. The so-called
HSVA tanker[2] was again chosen, as being the
best documented test case available, see
for instance Hoffmann[3] and Wieghardt and
Kux[4]. Even though measurement data have
been obtained only at model Reynolds num-
bers, the participants were asked, as an
optional exercise, to carry out calcula-
tions also for a full scale Reynolds num-
ber. This was to shed some light on the
difficulties encountered at this larger
scale, for which calculations have been
very rare, so far. The second test case
was designed to produce a significantly
different stern flow with a minimum change
of geometry . More information about the
design philosophy is given in the next sec-
tion. A very important feature of the se-
cond case (the "Mystery case") was that no
measurement data were available when the
calculations were carried out.

     As in the first Workshop, attention
was confined to double models, in which
wave effects are absent and the free sur-
face may be considered as a plane of sym-
metry. Also, only the flow on the bare
hull, without appendages and propulsors,
was considered.

     The first announcement of the "1990
SSPA-CTH-IIHR Workshop on Ship Viscous
Flow" was distributed in late 1988, to-
gether with a questionnaire to be returned
by 15 May 1989 by all researchers interes-
ted in taking part in the Workshop calcula-
tions. Efforts were made to invite parti-
cipation by originators of commercial CFD
codes. No less than 21 computors indicated
their interest in participating, and in
August the data and instructions for the
first test case were sent out. Similar in-
formation for the second case was distribu-
ted in December. In the early summer of
1990 results from 19 methods had been re-
ceived. and the difficult task of conden-
sing all the information into a uniform
format was started at CTH. By the time of
the Workshop meeting, which was held at CTH
12-14 September 1990, all results had been
plotted in a way such that comparison bet-
ween the different methods could be easily
made. Further, the replies to the question-
naire had been compiled at IIHR and conden-
sed into a table, useful for quick referen-
ce to the theory behind each method.

     In the present paper a brief summary
of the Workshop is given. The two test ca-
ses are described next, followed by an
overview of the methods. Thereafter, some
important results are discussed and finally
some conclusions are drawn. For a full ac-

count of the Workshop, reference should be
made to the Proceedings[5].

Test cases

HSVA Tanker, Case I

     A body plan of the first test case,
the HSVA tanker is shown in Fig. 1. The
boundary layer measurements by Hoffmann[3],
and the subsequent stern-flow measurements
by Wieghardt, Kux and Knaack[4], were made on
a double model of this hull in a 1.2 m dia-
meter, slotted-wall wind tunnel, in which
the turbulence level was of the order of 1
percent. Different types of pressure probes
were used. The model was supported in the
tunnel by means of wires and a sting at the
stern. The nominal length of the model was
2.74 m but for reference length we have
used the length between perpendiculars, L =
2.664 m, which gives a Reynolds number of
$5 \cdot 10^6$. Neither the tunnel nor the support
were modeled by any of the computors.

Mystery hull, Case II

     The second test case, for which no
measured data were available by the time of
the meeting, was designed by Prof G. Dyne
at Chalmers and Mr L.G. Jonsson at SSPA.
The purpose was to create a significantly
different wake pattern with a minimum of
geometry change as compared to the first
case. Thus, only the stern sections were
modified. By making them more U-shaped
stronger longitudinal vortices could be
expected behind the hull, creating a more
distorted wake field, see Dyne[6]. A body
plan is shown in Fig. 2.

     Velocity measurements using Laser-Dop-
pler Velocimetry were carried out at the
University of Hamburg after the Workshop[7],
but the results are analyzed and included
in the Proceedings[5].

Overview of methods

     Some 19 organizations from 12 count-
ries participated in the Workshop. A sum-
mary of the important characteristics of
the methods is presented in Table 1 (at
the end of the paper). This table was
prepared on the basis of information sup-
plied by the participants in a question-
naire that was distributed at the beginning
and again at the end of the Workshop. Ef-
fort was made to obtain as much and as
accurate information as possible on each
method. The following is a review of some
of the similarities and differences among
the methods.

     The overall strategy summarized in
item A indicates that 12 participants re-
stricted their calculations to the stern
and wake flow (S) while 7 treated the com-
plete hull (H), including the bow. Both
global (G) and zonal (Z) methods are repre-
sented but the most common combination is a
global method applied to the stern flow
(S,G). The 5 zonal approaches employ an
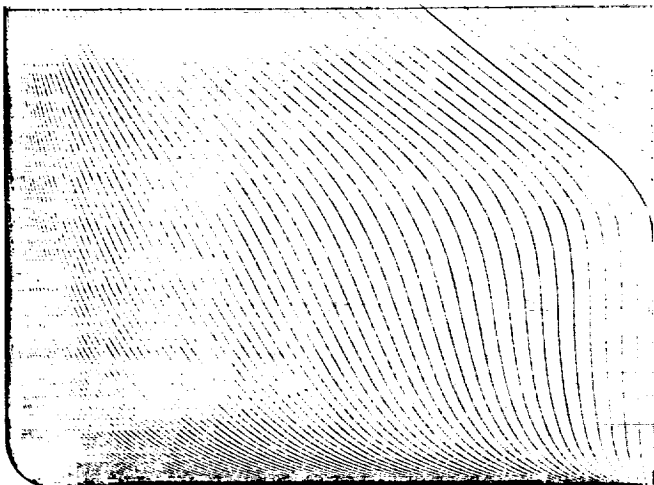inviscid-flow method. In three of these,
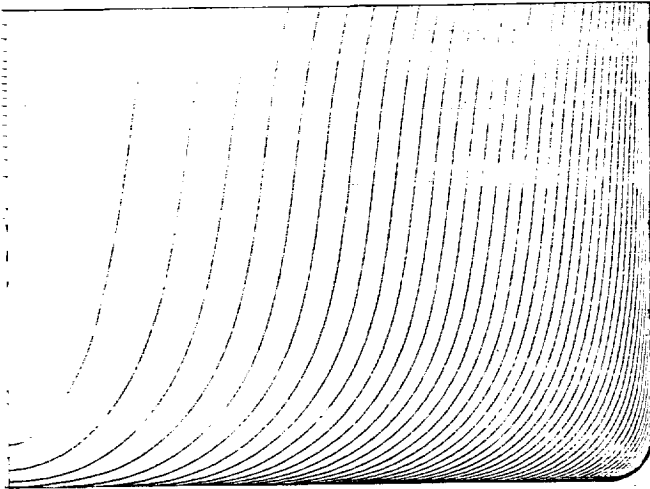
Forebody
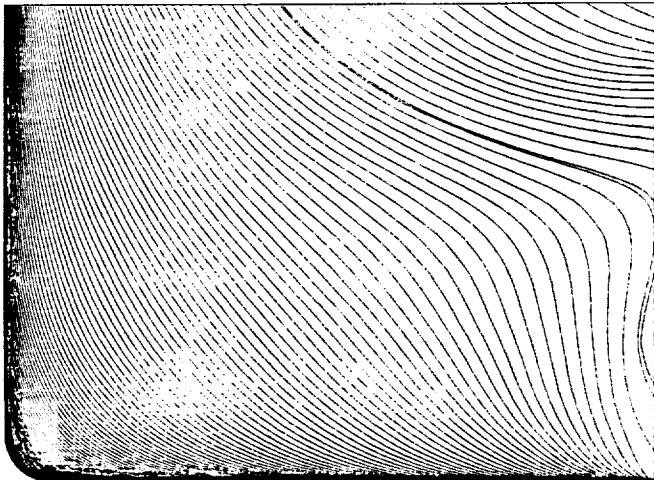
Afterbody

1. Body plan, HSVA Tanker

2. Body plan, Mystery Hull (Forebody as HSVA Tanker)

the viscous and inviscid solutions are matched at a specified boundary outside the viscous layer. One participant group (CT) made both global and zonal calculations. However, only the results from their global calculations are presented here. It is significant to note that none of the zonal approaches performed iterations between the viscous and inviscid flows to allow for interaction although in some cases the match boundary between the two zones was placed rather close to the hull.

Section B of Table 1 summarizes the equations and variables. One method employs integral equations and therefore provides a link to the earlier ship boundary layer Workshop[1]. It is clear that much of the information sought through the questionnaire is not relevant to the integral approach and therefore there are very few entries for that method. Among the differential methods, a vast majority solves the Reynolds-Averaged Navier-Stokes equations, while four adopt reduced forms (P, Ra) of these equations. One method uses large-eddy simulation along with a subgrid turbulence model. In all cases, the equations are solved in the so-called primitive variables, i.e., velocity and pressure. Thus, for example, methods that use vorticity or stream functions are not represented. There is a great deal of variability in the choice of the velocity components, ranging from simple, orthogonal ones to covariant components and grid-oriented nonorthogonal components. This choice impacts on the complexity of the codes and storage requirements for the geometrical quantities associated with the grid. Most methods employ nonorthogonal coordinates in all planes, but a few retain orthogonality in one (usually transverse) plane. This particular feature is related to the manner in which the grid is generated.

With the exception of the integral approach, all methods require a model for turbulence. These are summarized in section C. It is seen that 4 methods use algebraic models of eddy viscosity or mixing length (AL) and 13 employ the k-ϵ model. The large-eddy simulation method uses the Smagorinsky eddy-viscosity model along with the van Driest damping function for the subgrid scales. Of the 4 methods that employ algebraic, zero-equation models, three use the Baldwin-Lomax model and one (H) uses the mixing-length model. As far as can be ascertained, all users of the two-equation k-ϵ model retain the same constants, $(C_\mu, C_{\mu 1}, C_{\mu 2}, G_k, G_\epsilon) = (0.09, 1.44, 1.92, 1.0, 1.3)$. In two cases (HC, PV), however, the basic k-ϵ model is combined with a one-equation model for the near-wall region, while others employ the wall function approach. These two, and the methods employing algebraic models, integrate the flow equations up to the wall, where the no-slip condition is applied. This approach requires many more grid points in the near-wall region to resolve the large gradients of velocity and eddy viscosity. Methods using the wall-function approach,

on the other hand, satisfy the law of the wall and related conditions at one or more grid points away from the wall, and do not explicitly solve the flow equations in the near-wall layer.

Section D of Table 1 provides an overview of the boundary and initial conditions employed in the various calculations. As all methods approach the solution either by a time marching or an iterative process, all require initial conditions (time = 0). In this respect, three methods start the solution from rest, 7 use uniform flow, one uses boundary layer solutions, another uses a potential flow solution, while 5 indicate some other procedure. Among the last category are methods in which a parabolic march is made through the solution domain with an assumed initial pressure field. There is also considerable variation among methods in the quantities that are determined or prescribed at the start of the calculations. The initial conditions presumably influence the number of iterations or time steps required to obtain the steady state solutions that are sought.

The upstream boundary conditions depend upon whether the solution is obtained for the entire hull or only the stern and wake flow. In the case of the calculations for the entire hull, two types of treatment have been made. In five of the seven such calculations, the upstream boundary is placed about one-half ship length ahead of the bow, and quite simple boundary conditions are prescribed in the uniform flow there. In the remaining two (IL and KaO), the boundary layer over the bow is calculated. It appears that none of these calculations takes any account of the initial region of laminar flow or of the transition that was provoked artificially in the experiments. In the 12 calculations that were restricted to the stern and wake flow, there are differences in the location where the calculations were started as well as in the parameters that are prescribed. Three participants started the calculations at a check station, X/L = 0.646, where the integral parameters of the boundary layer were supplied from experiment. (The X-axis is along the hull, with the origin at the bow.) Others started the calculations somewhat ahead of this section, using, in some cases, the data at the check station as a guide. In all such calculations, however, the detailed velocity and turbulence parameter distributions required by the methods had to be generated by the participants. In this regard, most appear to have used two-dimensional boundary layer correlations, with the three dimensionality neglected. In one case (PJL), however, a special updating scheme was devised to obtain a set of initial conditions that is consistent with the equations being solved. The differences in the initial conditions are likely to be observed most clearly in the results at the check station.

There is also considerable variation in the location of the downstream boundary

where the solutions terminate, and the conditions applied at that boundary. In most cases the solutions are taken far enough from the stern to assume a negligible upstream influence and for the parabolic or extrapolated conditions to be valid.

The boundary conditions at the hull surface were discussed above in connection with the turbulence model. For completeness, however, we note that the no-slip conditions are applied explicitly in some methods whereas they are satisfied indirectly in methods that rely on the wall-functions approach.

All of the calculations presented at the Workshop have exploited the geometric symmetry about the ship centerplane and calculated only one half of the hull. Also, all participants assumed a double body and applied symmetry conditions along the water plane.

The location of the solution boundary in the "farfield" some distance from the ship axis, and the conditions specified along that boundary, also show considerable differences. With respect to the location, the five zonal calculations performed with viscous and inviscid methods use a boundary that varies from 0.08 of a ship length in one case (H) to 0.7 in another (KaO). Recall that this is the boundary at which the two solutions are matched and, as noted earlier, none of the calculations accounted for the interactions between the two regions. In these zonal calculations, the inviscid solutions provided the boundary conditions for the viscous solutions. In the remaining, global approaches, the location of the farfield boundary ranged from 0.1 of a ship length (T) to 1.5 (HC) with many using a value of one ship length. However, those who have used boundaries rather close to the hull (SZC and T) have provided boundary conditions from inviscid flow. In this respect, these methods, characterised as global by their originators, could also be regarded as zonal. Methods that have placed the boundary at larger distances from the hull have tended to prescribe uniform-flow conditions in the far field. Some differences are observed, however, in these cases in the particular variables or conditions that are specified or satisfied; see, for example, codes C and A in the table.

Section E of Table 1 pertains to the generation and control of the numerical grid. For the Workshop calculations, all participants employed a single block grid although one (GCHM) indicated that their method can accommodate a multi-block grid. Fully nonorthogonal grids as well as grids that are orthogonal in some planes (typically in the transverse sections) or at boundaries (usually at the hull) are represented in the calculations. The most popular method for generating the grid appears to be numerical, although some participants have employed analytic and algebraic methods, and even combinations of methods.

Among the numerical approaches, elliptic methods for the entire three-dimensional solution domain are the most common. Several methods use post-generation smoothing of the grid. Control of the grid is exercised most commonly from the boundaries although some indicate that it is done from inside the solution domain.

The numerical features of the various methods are summarized in section F. First of all, we note that there is no participation from the finite-element community and therefore items in the questionnaire that were designed specifically to obtain information on such methods are deleted in the table. Of the methods represented at the Workshop, there are four finite-difference methods, 10 finite-volume methods, and, for lack of a better term, four are classified as mixed methods. To these must be added the one based on integral equations which are also solved by finite-difference methods. It should be pointed out that not all of the methods in each of these categories are generically different. In other words, there are groups of methods in each class which share a great deal in common and, from a numerical perspective, may be classified as a single method. Be that as it may, we shall note the most significant features of the methods represented here.

First, discretization in both staggered and regular (colocated) grids is used in finite-difference as well as finite-volume methods. There is some correlation between the type of grid used and the method employed to solve for the pressure (or establish the pressure-velocity coupling) for this incompressible flow. Differencing of the convective terms is made by a variety of means, including upwinding, central differences, hybrid combinations and use of analytic solutions (FA). The responses to the questions on formal order of accuracy and formally conserved quantities are rather surprising. Most methods claim first or second-order accuracy but two consider their methods to be accurate upto the third order. The response to the second question seems to be correlated with the equations that are solved rather than any formal attempt in the methods to conserve mass, momentum, and total energy.

For the pressure, four methods use fully-coupled solutions. Two of these (GCHM and K) employ artificial compressibility, one (AS) uses a discretized continuity equation, another (H) uses the normal momentum equation. Most of the remaining methods employ segregated pressure-velocity coupling algorithms, SIMPLE being the most common.

In the execution of the solutions, most methods employ iterative techniques with under-relaxation or variable time steps. Explicit as well as implicit methods are represented. The solutions of the discretized algebraic equations are obtained using different tactics, including point substitution, line substitution, LU decomposition of matrices, and ADI methods.

Section G of Table 1 concerns the computations performed by the participants. As the two test cases are not substantially different with respect to the computational effort involved, the numbers in this section are typical of both cases. First of all, it is quite significant that calculations have been performed not only on state-of-the-art supercomputers (designated by S) but also on smaller machines (designated by M), such as workstations. The total number of grid points employed shows a great deal of variation, ranging from a low of 8,000 to a high of 253,000. It is interesting to note that the higher numbers are not necessarilly correlated with the use of supercomputers, nor are they correlated with the use of near-wall turbulence models or calculations made for the entire hull including the bow.

The number of time steps or iterations performed to obtain the solutions presented here varied widely, ranging from only 40 (BZLS and SZC) to 20,000 (ZM), although, in the latter case, the large-eddy simulation should never realize a steady state as defined for the other methods. It should be noted that a variety of convergence criteria were adopted to declare that a steady state had been obtained. The storage requirements and computer run times also varied over very wide limits. This is not surprising in view of the differences in the number of grid points and machines employed, but it is interesting to note that run times ranging from several hours to 5 days were reported by users of the smaller machines. The differences in the machines are also reflected in the cpu time per iteration per grid point. The fastest times were of course reported by users of supercomputers.

Results and Discussion

Results were requested from the participants at a Reynolds number of $5 \cdot 10^6$ for both hulls. As an optional exercise the computors were also asked to submit full scale results corresponding to a Reynolds number of $2 \cdot 10^9$ for case I. All but one delivered the model scale predictions but only three had computed the high Reynolds number case.

Pressure and friction distributions were reported at the waterline and keel and along three section girths on the hull, while velocity distributions in the form of iso-velocity contours and, in some cases, cross-flow vectors were given at four sections. For the most interesting section, the propeller plane, the pressure and (if computed) the turbulent kinetic energy were also reported.

The complete results may be found in the Proceedings[5], but in the present paper only a few representative examples will be given. These include the pressure distribution along three section girths and the velocity distribution (iso-velocities and
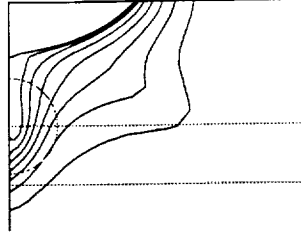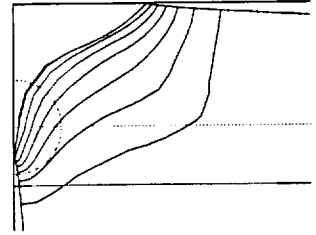
Abdallah & Sotiropoulos
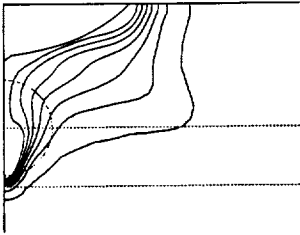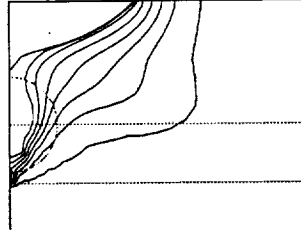
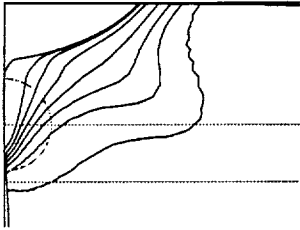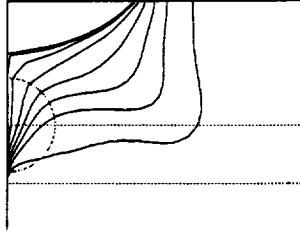Broberg, Zhang, Larsson & Schöön
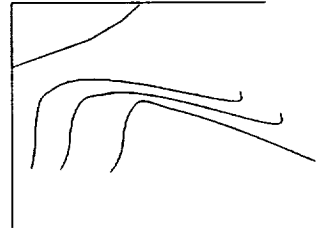
Bull, Watson & Musker

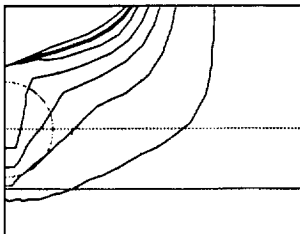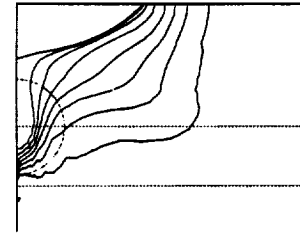Caprino & Traverso

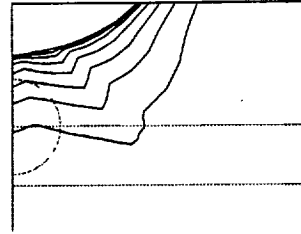Gorski, Coleman, Haussling & Miller

Hoekstra
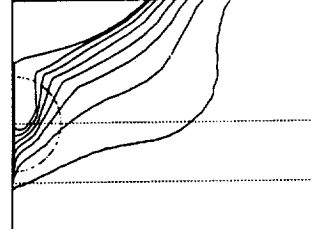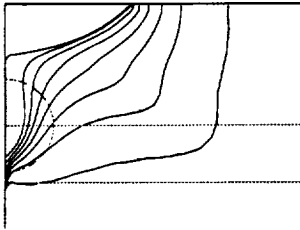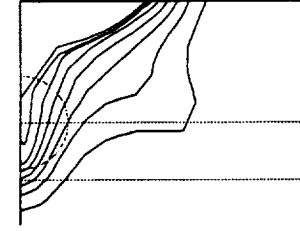
Hoffman & Chan

Ikehata & Liu
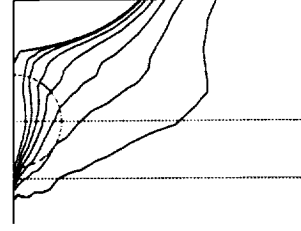
Kang & Oh

Kodama

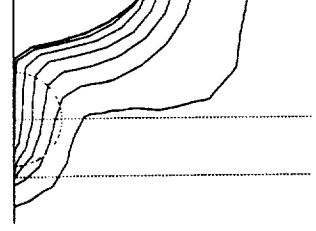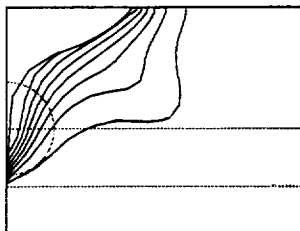Kanevsky & Orlov

Majumdar, Zhu & Rodi
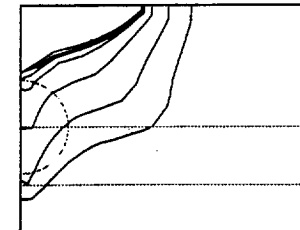
Masuko, Shirose & Abe

Patel, Ju & Lew

Piquet & Visonneau

Shen, Zhang & Cai

Tzabiras

Zhou & Gao

Zhu & Miyata

Legend:

exp   calc

o   —————— c_p at x/L=0.646

□   - - - - - c_p at x/L=0.875

△   - · - · c_p at x/L=0.942

3. Pressure distribution at three sections

Abdallah & Sotiropoulos

Broberg, Zhang, Larsson & Schöön

Bull, Watson & Musker

Caprino & Traverso

Gorski, Coleman, Haussling & Miller

Hoekstra

Hoffman &Chan

Ikehata & Liu

Kang & Oh

Kodama

Kanevsky & Orlov

Majumdar, Zhu & Rodi

Masuko, Shirose & Abe

Patel, Ju & Lew
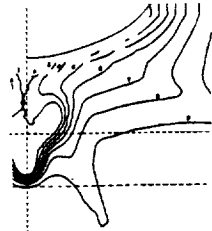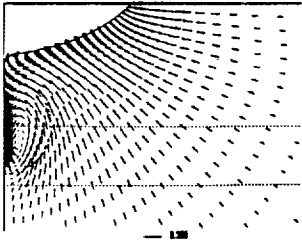
Piquet & Visonneau

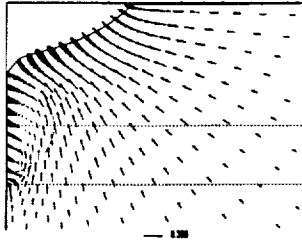Shen, Zhang & Cai

Tzabiras

Zhou & Gao

Zhu & Miyata

Experiment

4. Axial velocity contours at the propeller plane X/L = 0.976 (U/U_∞ = 0.3, 0.4, 0.5, 0.6, 0.7, 0.8, 0.9)
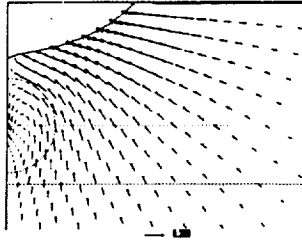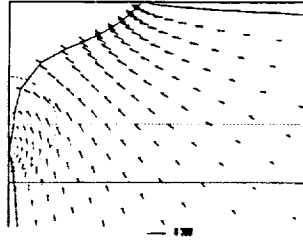
Abdallah & Sotiropoulos
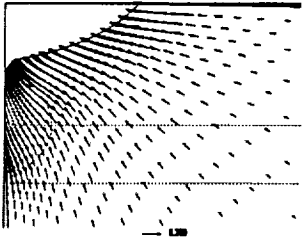
Broberg, Zhang, Larsson & Schöön

Bull, Watson & Musker
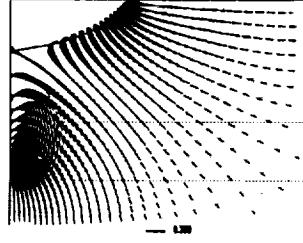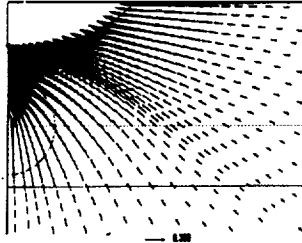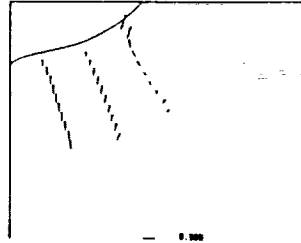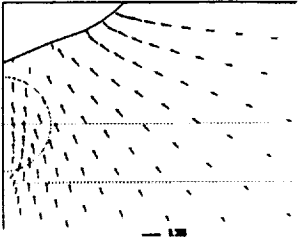
Caprino & Traverso

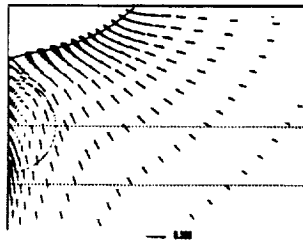Gorski, Coleman, Haussling & Miller

Hoekstra

Hoffman &Chan

Ikehata & Liu
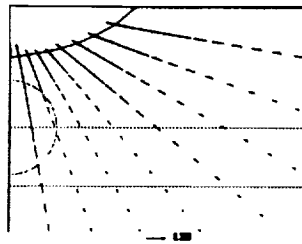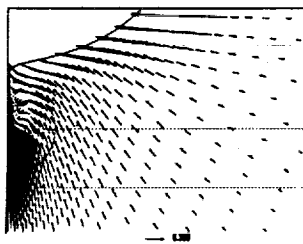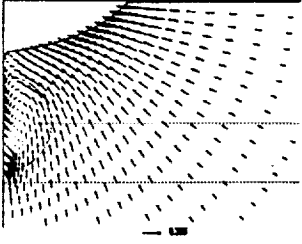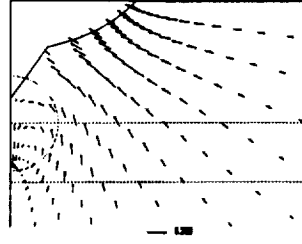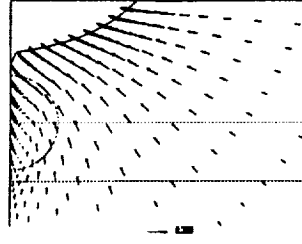
Kang & Oh

Kodama

Kanevsky & Orlov
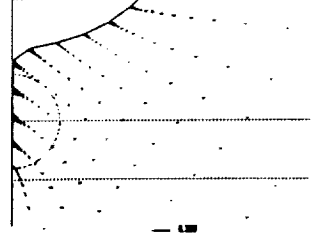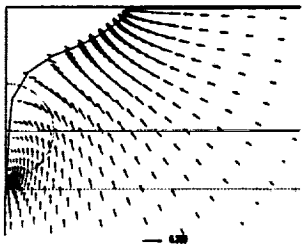
Majumdar, Zhu & Rodi
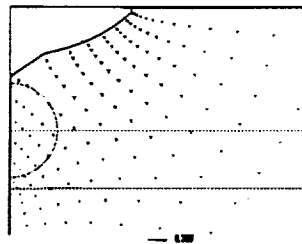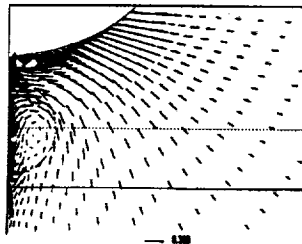
Masuko, Shirose & Abe

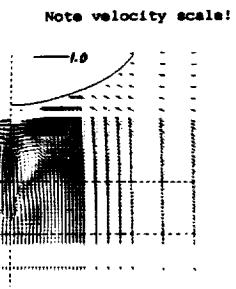Patel, Ju & Lew

Piquet & Visonneau

Shen, Zhang & Cai

Tzabiras

Zhou & Gao

Zhu & Miyata

Experiment

Note velocity scale!

5. Cross-flow velocity vectors at the pro-
peller plane X/L = 0.976

cross-flow vectors) at the propeller plane
of Case I, see Figs. 3, 4 and 5. In these
Figures the results of all 19 methods are
included. Measured data are represented by
symbols in Fig. 3, while the computed re-
sults are given as lines. In Fig. 4 iso-ve-
locity contours corresponding to 0.3, 0.4,
0.5, 0.6, 0.7, 0.8 and 0.9 times the undis-
turbed velocity are given. For comparison
the experimental data are shown in the lo-
wer right corner. Note the different scales
for the computed and experimental cross-
flow vectors in Fig. 5.

Before embarking on a more detailed
analysis a comparison of the results pre-
sented at this Workshop with those obtained
a decade ago for the SSPA-ITTC Workshop on
Ship Boundary Layers[1] is quite revealing.
Fig. 6 shows the axial velocity contours
for the HSVA Tanker at X/L=0.942 presented
at the previous Workshop. A comparison of
these with the results shown in Fig. 4 pro-
vides an overview of the achievements of
the past decade. It is clear that the ear-
lier boundary layer methods have given way
to those based on the Navier-Stokes equa-
tions. Only one such method was represented
in 1980. At the present Workshop, only one
boundary layer method was represented. The
question is whether or not real progress
has been achieved in the prediction of the
flow. If the contours of axial velocity at
the stern are used as the only measure of
success, then we may conclude that progress
has indeed been made. But, consider the
following observation. Most calculations
methods of the past did rather well at pre-
diction of the boundary layer over the hull
and failed only at the stern. Among the
present methods, few, if any, predict the
boundary layers with the same level of ac-
curacy but continue to provide results for
the flow over the stern and into the wake.

The girthwise pressure distributions
of Fig. 3, will be considered section by
section. First of all, we note that there
are significant differences in the way dif-
ferent methods obtained the results at the
check station, X/L = 0.646. As indicated in
item A of Table 1 (Code H), seven methods
performed calculations for the entire hull,
starting upstream of it. Although the man-
ner in which this was accomplished dif-
fered, their results at the check station
reflect, to some extent, their resolution
of the flow over the bow. Of the remaining
methods, three started the calculations at
the check station itself (see item D, Table
1) using the integral parameter information
provided there. Note that no information on
the crossflow at the check station was pro-
vided. The remaining methods started the
solutions on the hull somewhere upstream of
the check station and may have used the
information provided to guide the selection
of the upstream conditions. These differen-
ces among the methods must be taken into
consideration when examining the results at
the check station as well as further down-
stream.

In view of the foregoing, the results
of four of the seven methods that calcula-

Measured
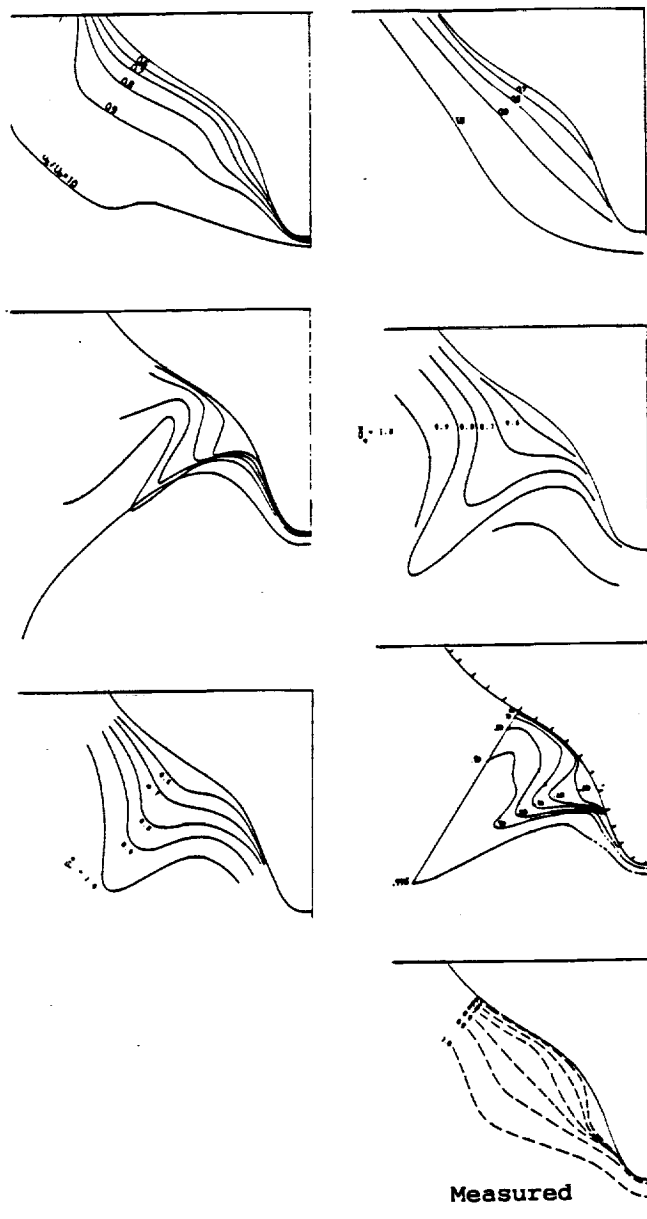
6. Axial velocity contours at X/L = 0.942,
predicted in the 1980 Workshop[1].

ted the flow over the entire hull are in
remarkably good agreement with the data
with respect to the girthwise pressure dis-
tribution at the first station. In fact,
their predictions are as good as those of
some of the methods that started the solu-
tions on the hull. Methods that started the
calculations on the hull show varying le-
vels of agreement in the pressure distribu-
tion at the check station. The disagreement
at the check station of methods that star-
ted at that station, or just upstream, are
rather surprising. The reasons for this are
not clear. Be that as it may, these diffe-
rences should be borne in mind as compari-
sons are made further downstream.

At the next downstream section, X/L
= 0.875, we see that the measured pressure
distribution shows a decrease from the

keel, with a minimum c_p of about -0.24 around 30 percent of the girth, an increase up to about 70 percent of girth, followed by a near constant value of -0.11 around the waterline. It is clear from Fig. 3 that many methods reproduce this trend but, with one possible exception, fail to predict either the magnitude or the location of the pressure minimum.

At the last section, X/L = 0.942, the measurements indicate minimum cp at around 8 percent girth, much closer to the keel than at the previous station, and an increase followed by a constant pressure around the waterline. The calculations generally predict higher pressures throughout and all fail to capture the dip in pressure around 45 percent girth. The methods that did poorly at the previous station continue to yield poor results at this station also.

From the point of view of propeller design the most interesting results are those at the propeller plane, reported in Figs. 4 and 5. The propeller disk is indicated in these Figures, and it is seen that particularly in this area the results vary considerably between the different methods. For classification purposes it is possible to distinguish between three types of results, see Fig. 7.

A   B   C
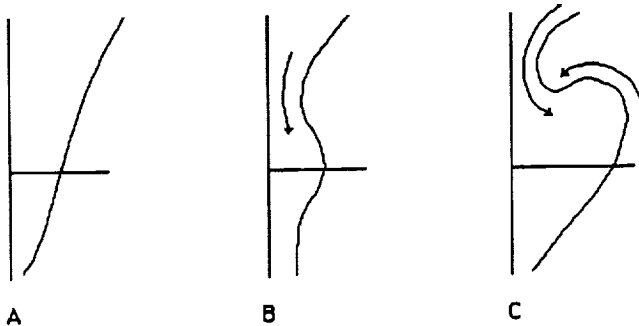
7. Different types of axial velocity contours at the propeller plane.

A.   V-shaped contours

B.   Contours with a bulge at or below the propeller center, indicating that part of the ship boundary layer has been displaced downwards by the longitudinal vortex hitting the propeller plane slightly above the propeller center (see Fig. 5).

C.   Contours with a pronounced "hook" due to the action of a stronger vortex.

Obviously the measured wake is of type C with quite distinct hooks in the 0.3 and 0.4 contour curves.

Investigating the contours of Fig. 5 it is seen that only one method produced a wake of type C, but the results of this method outside the propeller disk, particularly near the waterline, look quite unre-

alistic. Four or five methods predicted a wake of type B, while the remaining ones produced A type wakes.

For a propeller designer this situation is unsatisfactory, since the wake distribution determines the variation in loading during one turn of the propeller, i.e. the vibratory forces. On the other hand, as was shown by one of the authors (Larsson) at a continued Workshop in Osaka in the fall of 1991, the mean value around the circle at all radii may still be well predicted, as may the mean value of the velocity in the entire propeller disk. This means that the pitch and its distribution on the blades might be reasonably well predicted using the calculated wakes of the 4-5 best methods.

The reason for the failure to predict hook-like velocity contours was discussed extensively during the Workshop. To structure the discussion it was divided into four main themes: grid generation, equations and boundary conditions, turbulence models and numerical method.

There appeared to be a general consensus that grid resolution was not a major cause of the differences between, on the one hand the methods themselves, and on the other hand the measurements. This opinion was substantiated by the fact that several computors had carried out grid independence studies with very small changes in the results. There was however a general feeling that the resolution of the transverse pressure gradient was too low near the bilge (region of high transverse curvature) on the afterbody. Since this is where the longitudinal vortex is generated, the lack of resolution could explain the too-weak vorticity in the wake predicted by most methods. An impression of the grids used can be obtained from Fig 5, although, for clarity, not all the grid points are shown for some methods.

As for the governing equations, a difference not reported in the questionnaire turned out to be the way in which the turbulence terms are considered. It became clear that only a few methods include all of the terms. Another difference in the governing equations (appearing from Table I) is that some methods use the partially-parabolic approximation, while others are fully elliptic. This difference was discussed, and it was concluded that no correlation could be found between the approximation level in this respect and the performance of the method, as judged by the results reported. Some participants had in fact computed Case I using both types of equations and found very small differences.

Different inlet boundary conditions are required depending on whether the computational domain starts on the hull or upstream of it, but in all cases the participants were free to match their solution to the measured data at X/L = 0.646. Large differences are, however, seen at this sta-

tion, indicating that this possibility was not exploited by most of the computors. Instead, the boundary layer at the inlet station, if on the hull, seems to have been estimated from flat-plate correlations. The methods starting upstream use uniform inlet flow. To avoid numerical problems a nonzero value of the eddy viscosity had to be applied right from the start. Values of 50 to 100 times the laminar viscosity were mentioned. No attempt was made to consider transition. The general feeling was that the inlet conditions did not significantly influence the results at the stations on the afterbody and in the wake. This conclusion had in fact been verified by some participants.

Some discussers expressed the opinion that the only way to resolve details of the flow close to the wall (such as limiting streamlines) is to abandon the wall law. The general opinion was, however, that it is difficult to see a large difference in performance between the methods using the wall law and the others. A better prediction of the wake contours would have been expected, and this was achieved by some of the non-wall law methods but not all. It was pointed out also that virtually the only way to compute the full scale case is to employ the wall law, since otherwise the innermost grid points have to be positioned extremely close to the surface, giving rise to problems with the cell aspect ratios (the non-dimensional distance from the surface, y/L, is about 250 times smaller for the full scale case for a given value of $y+$). The other boundary conditions were considered relatively unimportant for the problems at hand.

Different opinions on the general importance of turbulence modeling were expressed. It was argued that as experiments have indicated that the Reynolds stresses are very small in the major part of the viscous region near the stern, even an inviscid calculation might produce a reasonable result. Some participants reported on earlier computations for axisymmetric and three-dimensional bodies, where this approach had been tested with relatively good results. Obviously the inviscid region had to be restricted to the neighborhood of the stern.

A possible explanation for the failure to predict the correct wake contours might be the inability of the methods to resolve the pressure field accurately, i.e. to predict the transverse pressure gradients that are believed to produce the vortical flow structure. In this case, a number of numerical issues are involved, including the grid arrangement used (staggered versus regular) and the manner in which the pressure is calculated.

Conclusions

The Workshop clearly showed that great progress has been made during the 1980's in the development of methods for predicting the flow around the stern and in the near wake of ships. The boundary layer based approaches of the 1980 Workshop have given way to methods based on the Reynolds-Averaged Navier-Stokes equations, albeit using relatively simple turbulence models. While the former methods either broke down before, or predicted completely unrealistic results in the propeller plane, the new methods in general capture the gross features of the wake, such as the thin shear layer in the lower part and the piling-up of boundary layer low speed flow around half draught. In fact, the best methods of the Workshop predict the shape and location of the velocity contours in most of the propeller plane with reasonable accuracy. The results are however less satisfactory in the central part of the wake, i.e. inside the propeller disk. The bilge vortex, although weak, redistributes the low speed flow from the boundary layer in such a way that very uneven hook shaped velocity contours are created. This feature is missed to varying degrees by the different methods. Various reasons for this were discussed during the Workshop, but no definite answer could be given. One possible explanation is that the large velocity and pressure gradients in the bilge region are too inaccurately resolved in the grids employed.

There are no general differences in performance between methods based on zero equation turbulence models as compared to the two equation models. The disadvantages of the simpler models may be outweighed by the advantages of computing the flow all the way down to the surface. Two equation models are usually employed in combination with the wall law.

Although the new methods are superior to the old ones in predicting the wake, results from calculations starting upstream of the hull, or in front of the check station, indicate that the ability to predict the thin boundary layer has not been improved, rather the contrary. The likely reason for this is grid resolution. To save computer time very few grid points are located in the thin boundary layer on the forebody, where the much faster boundary layer methods may use grids with a very high resolution. This suggests a zonal approach where the expensive Navier-Stokes method is used in the stern and wake region while an efficient boundary layer method is used for the rest of the hull.

A final point to note is that most methods predicted, at least qualitatively, the differences between the two test cases. The computed cross flow for the second case is considerably larger in the propeller disk than for the first case, as the measurements have indicated, and the change in the contours of axial velocity also shows the right trend.

Acknowledgements

References

1   Larsson, L., (ed.) "SSPA-ITTC Workshop on Ship Boundary Layers 1980: Proceedings," SSPA, Goteborg, Sweden, Report No. 90, 1981.

2   Collatz, G., "Geosim Tests with a Model of Large Fullness," (in German) Forschungszentrum des Deutschen Shiffbaus, Report 28, Hamburg, 1972.

3   Hoffmann, H.P., "Investigation of the Three-Dimensional Turbulent Boundary Layer on a Double Model of a Ship in a Wind Tunnel," (in German) Inst. Schiffbau, Uni. Hamburg, Report 343, 1976.

4   Wieghardt, K. and Kux, J., "Nominal Wakes Based on Wind Tunnel Tests," (in German) *Jahrbuch der Schiffbautechnischen Gesellschaft (STG)*, 1980, Springer-Verlag, pp. 303-318.

5   Larsson, L., Patel, V.C. and Dyne, G., (ed.) "Ship Viscous Flow - Proceedings of the 1990 SSPA-CTH-IIHR Workshop", FLOWTECH, Gothenburg, Sweden, Research Report No 2, 1991.

6   Dyne, G., "A Study on the Scale Effect of Wake, Propeller Cavitation and Vibratory Pressure at the Hull of Two Tanker Models", *Trans SNAME*, 1974

7   Denker, J., Knaack, T. and Kux, J. "Experiments and Numerical Investigation of the HSVA2 Tanker (Second Test Case of the 1990 SSPA-CTH-IIHR Workshop), Inst. Schiffbau, Uni. Hamburg, Report 516, 1991.

Table I is found on the following 3 pages.

Table I

SUMMARY OF COMPUTATION METHODS
INFORMATION FROM RESPONSES TO QUESTIONNAIRE

Authors >>	AS	BZ LS	BW M	CT	GC HM	H	HC	LL	KO	K	KaO	MZ R	MS A	PL	PV	SZ C	T	ZG	ZM
A. OVERALL STRATEGY																			
INDICATE whether you calculate the complete hull (by H), or only the stern and wake flow (by S)	S	S	S	H	S	S	S	H	S	H	H	H	H	S	S	S	S	S	H
GLOBAL (single method is used for entire flow) (G)	G	G	G	G	G	G	G		G	G		G	G	G	G	G	G	G	G
ZONAL (separate methods are used in different regions; matched or patched) (Z); [* indicates combinations]		Z		Z*		Z		Z	Z		Z								
Matching along a specified boundary outside the viscous layer (P); INVISCID METHOD used (I)		PJ		P,J*		PJ		PJ			?,I								
B. EQUATIONS SOLVED																			
A PRIORI or DE FACTO APPROXIMATIONS	R	R	R	R	R	P	R	I	R	P	P	R	R	R	R	Ra	R	P	L
VARIABLES: Velocity and pressure (VP); etc.	VP	VP	VP	VP	VP	VP	VP	I	VP	VP	VP	VP	VP	VP	VP	VP	VP	VP	VP
Choice of components of vector quantities	2	6	2	5	1	M	1	3	2	1	2	1	1	2	1	6	3	2	1
COORDINATES (see also GRID)	3	3	3	3	3	2	3	0	3	3	3	3	3	3	3	2	?	3	3
C. TURBULENCE MODEL	AL	kε	kε	kε	AL	AL	kε k	I	kε	AL	kε	kε	kε	kε	kε k	kε	kε	kε	SG
Near-wall treatment	NS	WP	WP	W	NS	NS	NS		W	NS	?	W	W	WP	NS	W	W	W	NS
Number of turbulence-model equations solved	0	2	2	2	0	0	2	0	2	0	2	2	2	2	2	2	2	2	0
D. BOUNDARY AND INITIAL CONDITIONS																			
INITIAL (time = 0) From rest (O), uniform flow (1) ...	0	5	5	2 4	1	5	5		1	1	1	1	1	5	1	5	4	1	0
Variables determined in the above manner	1	2	3	3	1	0	3		3	7	7	2	3	2	3	1	?	0	?
UPSTREAM Location (x = 0 is bow, x = L is stern) x/L =	.5	.5	.3	.2 -.51	.646	.5	.5	.05	.5	-.5	.1 -.5	-.51 -.5	-.5	.3	.5	.5	.646	.5	-.5
Variables specified	2	1,3	2,3	0,3	0,2	2	.5	1	1,3	0,2	1	2,3	0,2	1	1	0,2	1	1	0,2
Conditions specified (2D b.l. flow, ...)	2	1,2	0,2	0 3	2	2	4	2	2	2	2,3	0	0	(3)	3	1,3	3	2	2
DOWNSTREAM Location, x/L =	1.8	2.0	5.	3.92	1.4	1.35	1.5	1.5	2	1.5	<1	1.6	2	4.5	2	2.5	1.25	1.8	2.
Conditions specified	B	B	B	AI	D,E	AI	A		A	A		A	A	B	A	A	E,A	A	?

Note: If ZONAL, complete the remainder for each viscous-flow region, carefully denoting the region to which the description applies. If a VISCOUS-INVISCID interaction method is used, indicate INTERACTION LAW: Displacement thickness (D); Surface and wake blowing or suction (S); Matching along a specified boundary outside the viscous layer (P); INVISCID METHOD used (I)

A PRIORI or DE FACTO APPROXIMATIONS — Note: Direct Simulation: no turbulence model (N); Large Eddy Simulation: NS equations with sub-grid model (L); Reynolds-averaged NS equations (R); RANS with grid-related approximations (e.g., nonorthogonal viscous terms neglected) (R-); Partially-parabolic RANS (longitudinal diffusion neglected; RANS with FLARE etc) (P); Thin-Layer RANS (only wall normal diffusion retained) (T); Boundary-layer equations (D: differential; I: integral)

VARIABLES — Velocity and pressure (VP); Velocity and vorticity (VV); Stream function and vorticity (SV). Choice of components of vector quantities [indicate by number(s)] Cartesian (1), cylindrical (2), other orthogonal (3), contravariant (4), covariant (5), grid-line oriented physical (6), mixed (M), other (7)

COORDINATES — Nonorthogonal in all planes (3); Nonorthogonal in two planes (2); Nonorthogonal in one plane (1); Orthogonal in all planes (0); Other (finite elements, etc.) (A)

C. TURBULENCE MODEL — None (N); Sub-grid (SG); Algebraic eddy-viscosity or mixing-length (AL); One-equation (e.g., k); Two-equation (e.g., k,ε); Algebraic stress equations (AS); Reynolds stress equations (RS); Other (e.g., integral equations, 1) Note: combinations indicated by two symbols (e.g., k ε, k). Near-wall treatment: No-slip (NS); Law of the wall: with pressure-gradient (WP), without (W)

D. BOUNDARY AND INITIAL CONDITIONS — INITIAL (time = 0) From rest (O), uniform flow (1), potential flow (2), boundary layer solutions (4), other (5). Variables determined in the above manner: Code - 0: p; 1: p, V; 2: V, k, ε; 3: p, V, k, ε

UPSTREAM: Variables specified (e.g., C_f, δ, u, v, w, p, k, ε, v_t, ...) Code - 0: p; 1: integral parameters; 2: V; 3: V, k, ε. Conditions specified (e.g., uniform stream, 2D b.l. flow, ...) Code - 0: uniform stream; 1: inviscid flow; 2: 2DBL; 3: 3DBL

DOWNSTREAM: Conditions specified Code - A: $p_\xi, \phi_\xi = 0$; AI: $p_\xi = 0$; B: $p_\xi, \phi_{\xi\xi} = 0$; C: V_{extrap}; D: p_{extrap};

	NS	WF	WF	WF	NS	NS	WF	NS	WF	WF	WF	WF	NS	WF	WF	WF	NS
WALL: No-slip (NS); wall function (WF)	S	S	S	?	S	S	S	—	S	S	S	S	S	S	S	S	S
WAKE CENTER — Conditions Specified: S: Symmetry	S	S	S	S	S	S	S	S	S	S	S	S	S	S	S	S	S
FREE SURFACE Double body, plane of symmetry	S	S	S	S	S	S	S	S	S	S	S	S	S	S	S	S	S
Conditions specified exact w/ boundary-fitted grid	S	S	S	S	S	S	G	S	B	S	S	S	S	B	S	S	S
FAR FIELD Location, R/L	.5	.3	1.	375	.08	1.5	>.5	1.	.7	51	5	1.	1.	.15	.1	3	?.5
Tunnel/tank (T), uniform stream (U), inviscid (I)	U	U	U	I	U	I	U	U	U	U	U	U	U	I	U	I	?
Parameters specified	B	C_1	C_2	C_2	B	B	B	C_1	C_1	C_1	C_1	C_o	C_1	B	B	B	A_2
Conditions specified	A_1	K_1	A_2	—	—	—	K_2	—	K_1	S	S	K_1	K_1	K_1	—	A_2	A_2
E. GRID — TYPE Single (SB) / multi-block (MB)	SB	SB	SB	MB	SB	SB	SB	SB	SB	SB	SB	SB	SB	SB	SB	SB	SB
Nonorthogonal (N)/planes (P)/boundaries (B)/everywhere (O)	N	N	P	N	P	N	N	N	N	N	N	N	N	P	B	N	N
GENERATION METHOD Analytic (A), numerical (N), algebraic (L)	N	N	L	A,N	A,L	N	N	N,L	N	N	N	L	N	L	A	N	N,L
Elliptic (E), hyperbolic (H), parabolic (P), transfinite (T), conformal (C), geometrical (Q)	E	E	T	C	C,T	E	Q	?	T	E	E	E	E	G	C	E	E
3D (3), 2D plane by plane (2), other (1)	2	3	3	2	2	3	3	3	3	3	3	3	3	3	2	3	3
Post-generation smoothing? yes (Y), no (N)	N	Y	N	N	N	N	N	Y	Y	N	N	N	N	Y	N	N	Y
CONTROL Adaptive? yes (Y), no (N)	N	N	N	N	N	N	N	N	N	N	N	N	N	N	N	N	N
Control from boundaries (B), from inside (D)	B	B	B	—	B	B	—	—	D	D	—	D	D	D	B,D	—	—
F. NUMERICAL METHOD — GENERAL CLASSIFICATION	FD	M	FV	FV	FD	FV	I	FV	FD	FV	FV	FV	M	FV	FV	FD	FV
DISCRETIZATION	R	S	S	V	R	R	S	R,V	S	S	S	S	R	S	S	T	S
DIFFERENCING OF CONVECTIVE TERMS	U	FA	FA	U	U	O	C,U	C,U	C,D	O	H	C,U	FA	O	H	U,C	H
FORMAL ORDER OF ACCURACY	2	M	M	3	2	2	M	2	1	1	1,2	1,2	M	M	1,2	2	3
FORMALLY CONSERVED QUANTITIES	M	Q	J	M	M	M	M	M	J	M	M	M	Q	M	J	M	M
LINEARIZATION	—	P	—	N	N	N	O	N	P	P	—	O	—	O	—	N	N
PRESSURE-VELOCITY COUPLING	O	—	—	A	O	—	A	—	?	—	—	—	—	—	—	—	?

NO FINITE-ELEMENT METHOD REPRESENTED

WALL: No-slip (NS); wall function (WF)

WAKE CENTER
Conditions Specified: Code - S: Symmetry [$U_n = 0$, $\partial(U_t, U_s, p,...)/\partial n = 0$)]

FREE SURFACE
Double body, plane of symmetry (S), exact with fixed grid (G),
exact with boundary-fitted grid (B), approximate (A, describe)

Conditions specified exact with boundary-fitted grid (B),
approximate (A, describe)

FAR FIELD
Location, R/L (or equivalent distance from axis) =

Tunnel/tank wall (T), uniform stream (U), inviscid flow (I)

Parameters specified: Code - B: (p, U^1, $U^2_{derived}$; C_1: $U^1 =1$, $\partial U^2/\partial n = 0$
C_2: $U^1 =1$, $U^3 =0$, $p=0$; C_3: U^1, U^2, U^3, p;

Conditions specified: Code - A_1: $\rho_n =0$, $\partial^2 U/\partial n^2 = 0$; A_2: $\partial(\rho, U^i)/\partial n = 0$;
K_1: $\partial(t, e)/\partial n = 0$; K_2: $(k, \varepsilon) = 0$; S: symmetry

E. GRID

TYPE
Single block (SB) or multi-block (MB)?

Nonorthogonal everywhere (N), orthogonal in planes (P), orthogonal at some
boundaries (B), orthogonal everywhere (O)

GENERATION METHOD
Analytic (A), numerical (N), algebraic (L)

Elliptic (E), hyperbolic (H), parabolic (P), transfinite (T), conformal (C), geometrical (Q)

3D (3), 2D plane by plane (2), other (1)

Post-generation smoothing? yes (Y), no (N)

CONTROL
Adaptive? yes (Y), no (N)

Control from boundaries (B), from inside the domain (D)

F. NUMERICAL METHOD

GENERAL CLASSIFICATION
Finite-element (FE), finite-difference (FD), finite-volume (FV),
Spectral (S), Integral (B), mixed (M), Other (O)

DISCRETIZATION
Finite-difference, regular or collocated grid (R); finite-difference, staggered grid (T);
finite volume, regular grid (V); finite-volume, staggered grid (S); finite element (L);
hybrid (H) & other (O), specify

DIFFERENCING OF CONVECTIVE TERMS
Centered (C); upwind, standard (U); upwind, skewed (K); rotated (A); explicit artificial viscosity (D);
hybrid, specify (H); other, specify (O) Code - finite-analytic (FA)

FORMAL ORDER OF ACCURACY (Convective terms)
First (1); second (2); third (3); fourth (4); mixed (M); other (O)

FORMALLY CONSERVED QUANTITIES
Mass (Q): mass and momentum (M); mass, momentum, kinetic energy (J); mass, momentum,
total energy (W); other (O) Note: There is some confusion here about conserved quantities

LINEARIZATION: Picard (P); Newton (N); Quasi-Newton (Q); Other (O)

PRESSURE-VELOCITY COUPLING
Fully-coupled solutions: direct method (D); penalty method (P); compressible-flow code
used at low Mach number (C); artificial compressibility (A); other (O)

Segregated: Poisson equation, e.g., capacitance techniques (P); pressure-correction technique, e.g., SIMPLE, SIMPLER, SIMPLEC, PISO, saddle-point method, preconditioning (C, list); other (e.g., boundary-layer type code) describe (O)
Code - S_1: SIMPLE; S_2: SIMPLER; S_3: SIMPLEST; S_4: SIMPLEC; P: PISO

ACCELERATION OF ITERATIVE SOLUTIONS
If you distinguish more than one iteration process in your method, classify them and specify the following for each of them: Under-relaxation (U); over-relaxation (R); grid sequencing (G); (U) on p only; multi-grid (M); additive terms (e.g., quasi-time dependent, fixed or variable time step)(A); conjugate gradient methods (C); other, describe (O)

STRATEGY
Explicit (E); implicit (I); semi-implicit (S); fractional step (F); other (e.g., optimal control, Newton-Raphson), describe (O)

TACTICS
Point substitution (P); line substitution (L); direct matrix inversion (M); Split (ADI-like); incomplete LU decomposition (D); other, describe (O)

G. COMPUTATIONS
Computer used, list
Code - S_1: CRAY YMP; S_2: CRAY XMP; S_3: CRAY 2; S_4: FACOM VP400; S_5: FACOM VP50
M_1: DEC 2100; M_2: FPS 264; M_3: MICROVAX 3800; M_4: Apollo 10000; M_5: SUN 4WS;
M_6: STELLAS WS; M_7: BESM6; M_8: IBM 3031; M_9: SPARC330; (Note: S for super; M for other)

Number of grid points used in axial and transverse directions:

Total number of grid points, thousands (K)

For above grid, storage utilized (MW: megawords
MB: megabytes)

For above grid, cpu time: m: min; h: hours; d: days

For above grid, number of iterations or time steps required for convergence, in thousands (K)

Convergence criteria employed
Code - NE: no explicit criterion; O: other

	A	B	C
1	$\Delta p < 5\,10^{-3}$	$\Sigma S < 10^{-3}$	$\Delta u < 10^{-4}$
2	$5\,10^{-4}$	$5\,10^{-4}$	
3	10^{-4}	10^{-5}	
4		$5\,10^{-5}$	

Approximate cpu per iteration per grid point, in 10^{-5} secs

Maximum grid that can be accommodated on the computer in thousands (K)

Number of grid points used in the region
$0.65 < X/L < 1.0$, $n^+ > 100$, $n/L < 0.1$ axial
                                                      radial
                                                      girth

Total number of grid points in the above region, thousands (K)

AUTHORS CODE

AS: Sotinopoulos & Abdallah, Uni. Cincinnati, USA
BZLS: Broberg, Zhang, Larsson & Schoon, Flowtech, Sweden
BWM: Bull, Watson & Musker, ARE-Haslar, U.K.
CT: Caprino & Traverso, CETENA, Italy
GCHM: Gorski, Coleman, Haussling & Miller, DTRC, USA
H: Hoekstra, MARIN, The Netherlands
HC: Hoffman & Chen, ARL, Penn State Uni. & Rockwell, USA
IL: Ikehata & Liu, Yokohama Nat. Uni., Japan
KO: Kang & Oh, Seoul Nat. Uni., & Kyungnam Uni., Korea
K: Kodama, Ship Res. Inst., Japan

KaO: Kanevsky & Orlov, Krylov, USSR
MZR: Majumdar, Zhu & Rodi, NAL, India & Uni. Karlsruhe, Germany
MSA: Masuko, Shirose & Abe, IHI, Japan
PJL: Patel, Ju & Lew, IIHR, Uni. Iowa, USA & Daewoo, Korea
PV: Piquet & Visonneau, ENSM Nantes, France
SZC: Shen, Zhang & Cai, MARIC, China
T: Tzabiras, Nat. Tech. Uni., Greece
ZG: Zhou & Gao, CSSRC, China
ZM: Zhu & Miyata, Uni. Tokyo, Japan

Category	Values (left → right)
Segregated code	--- S_2 S_3 / --- --- P / --- S_1 --- / S_1 S_1 S_1 / S_1 S_1 S_4 ?
Acceleration	U/A, A/A, R, U/O (G,U), C, ---, U, ---, U, U, U, A, A
Strategy	E, I, S, I, S, I, I, I, I, I, I, S, E,S
Tactics	P, L, L, O, D, P,D, D, L, Split, L, D, P, L, L, P,L, L, P
Computer used	S_y M_d M_j M_f S_x S_a M_a / M_i M_a M_b S_{f2} S_n / S_y S_2 M_i M_p M_i M_a
Grid (axial)	57 60 93 63 65 113 92 / 58 81 50 124 133 / 50 80 36 45 80 120
Grid (radial)	41 33 40 16 33 55 86 / 25 27 10 44 25 / 30 40 20 29 15 30
Grid (girth)	33 25 21 25 49 35 32 / 16 31 20 32 29 / 15 21 12 62 20 30
Total grid points (K)	79 49 78 25 105 218 253 / 23 68 10 175 96 / 23 67 8 81 24 108
Storage	MW 2.4 ... ; MB 6 24 11 3 1 --- 20 --- 63 30 12 1.8 0.2 --- 0.4 56
cpu time	90m 2h 30h 10h 9h 80m 20h / 3h 50h 30h 11m 2h / 10m 4h 5h 3h 3h 5d
Iterations (K)	4. .04 1.6 .3 2.5 .035 1. / .13 5. .1 .4 / .16 .3 .04 .06 .06 20.
Convergence	A_3C NE NE NE A_1 B_1 --- / B_1 NE --- B_2 B_4 / NE A_3C C B_3 A_2 A_3
Approximate cpu	2 500 92 11.4 29 / 388 50 3.9 13 16 50 / 2780 615 625 20
Maximum grid (K)	--- 300 120 --- --- / --- 123 705 500 112 1000 / --- --- 32 110
Region axial	33 / 30
Region radial	20 / 20
Region girth	25 / 21
Total region (K)	16.5 / 12.6